

# QSolar - A Tool to Generate Maps of Direct Sun Radiation

Johannes Rauh<sup>1</sup>, Martin Meister<sup>1</sup>, Reiner Suck<sup>2</sup>, Günther Greiner<sup>1</sup>  
meister@informatik.uni-erlangen.de

<sup>1</sup>Lehrstuhl Graphische Datenverarbeitung, Universität Erlangen-Nürnberg

<sup>2</sup>Institut für Vegetationskunde und Landschaftökologie (IVL)

<sup>1</sup>Am Weichselgarten 9, 91058 Erlangen

<sup>2</sup>Georg-Eger-Straße 1b, 91334 Hemhofen

## Abstract

For the description and classification of vegetation it is important to evaluate the local characteristics of the biological habitat. The German ministry of conservation's PNV project sets out to estimate the potential natural vegetation (PNV, [1]) of Germany that would be expected to evolve if human interaction ceased. In a student project we work in cooperation with biologists to investigate one of the abiotic factors influencing habitats. Direct sun radiation is one of the most important aspects of plant growth and habitat development. Depending on terrain features, surrounding landscape, latitude and atmospheric absorption we calculate a good approximation to the direct sun radiation received at ground level.

## 1 Introduction

Bavaria is the south-eastern part of Germany and covers nearly 71,000 km<sup>2</sup> (latitude 9 – 14, longitude 46 – 51 degrees). With its lowest height at 107 m (Kahl am Main) and the highest peaks in the Alps (Zugspitze, 2,962 m) it features interesting terrain features. In 2005 the computer graphics group and IVL set up an interdisciplinary student project to combine PNV project data and computer graphics approaches to implement a tool to compute maps of direct sun radiation. Different periods of time can be observed (e.g. vegetational period) for the mapping of the *sun hours*. A sun hour is counted when the amount of received energy exceeds  $200 \frac{\text{W}}{\text{m}^2}$  in an hour. Regions of arbitrary size are selectable as domains for the computations and an import/export into standard GIS software is provided.

## 2 Overview and related work

The position of the sun and its influence on the earth have been extensively studied since ancient times. In this paper we will focus on our technique of approximating solar energy interaction with terrain and the resulting shadowing for arbitrary terrain data. A detailed discussion of the determination of the position of the sun at a given time and space or

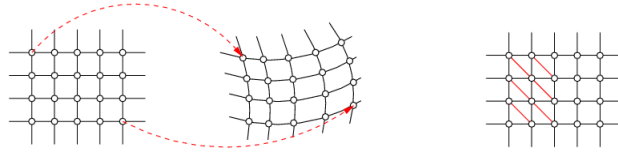


Figure 1: Change of geometry, constant topology. Right: regular triangulation scheme

different projection mappings are beyond the scope of this paper and we refer the reader to the literature ([2], [3], [4]).

### 3 Input data

We work with height data given as a 2D array representing Gauss-Krüger coordinates (German Grid, a mercator projection). The example dataset of Bavaria has a resolution of  $7,200 \times 8,000$  grid points (grid size  $\approx 50$  m). One of our first tasks is to remap the given grid to true 3D space coordinates (for details see [2]). To facilitate a fast lookup of neighbours we keep the vertices in memory along the original organisation of the grid (topology). These 3D coordinates of our model of the earth are intuitively situated in space where they are illuminated by the sun's (parallel) rays. At each vertex  $v$  normals for our terrain can be estimated using the given topology (figure 1, right). The ellipsoidal normal  $\vec{s}_v$  is a normalized vector normal to the tangent plane of the Bessel ellipsoid at a surface point.

### 4 Diffuse radiation

Our model to determine the amount of radiance received by terrain (assumed total diffuse reflector) is Lambert's cosine law. The normalised light vector  $\vec{L}$  and normalised surface normal  $\vec{n}_v$  of vertex  $v$  yield  $E_{\text{Lambert}}(\vec{L}, v) = \langle \vec{L} | \vec{n}_v \rangle = \cos(\phi)$  with  $\phi$  being the angle between the two vectors. To decide whether the two vectors enclose an angle greater than  $|90|$  degrees (light hits the back face of the terrain) we test for the sign of the scalar product. This lambertian term provides us with an upper boundary for the maximum energy available.

### 5 Shadowing

We can make the shadow computation efficient by traversing the grid in a suitable way. To avoid testing much of the same geometry again we re-use shadow information. Introducing a quick *early reject* and *early accept* for shadow, we test the shadow information of the two neighbours in light direction. These can be quickly found based on the assumption that our topology information can be used for our transformed geometry. Starting the computation from the boundary vertices and working inwards by using a grid-walk best suited for the current light direction (we distinguish eight directions, see figure 2) all points are already

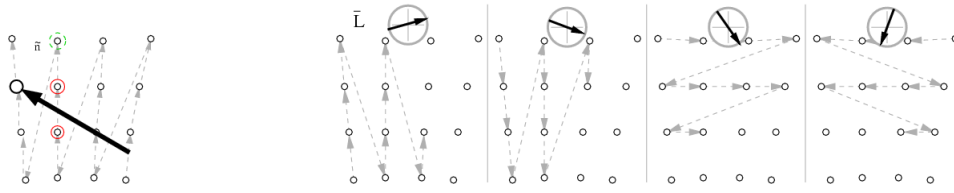


Figure 2: Left: Grid with processing order and light vector showing the two neighbours used for the early accept/reject tests, right: Four of the eight directions

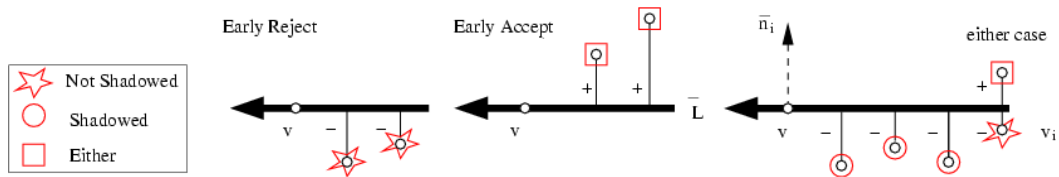


Figure 3: Shadow tests: left and middle easy cases, right complex case (both configurations for final decision shown)

processed that can contribute to the shadowing of the current vertex. The shadow lookup is done by examining the distance of the nearest vertices  $v_i$  in light direction when projected on a plane defined by the position of the current vertex  $v$  and the light vector with a normal  $\vec{n}_l$  (see figure 3). Distances smaller than 0 are below the plane and do not cast a shadow, distances greater than 0 will shadow the current vertex.

$$d = \langle \vec{n}_l | (\vec{v}_i - \vec{v}) \rangle = \begin{cases} \leq 0 & : \text{ does not cast shadow} \\ > 0 & : \text{ casts shadow} \end{cases}$$

Early accept is reached when the neighbours cast shadow on the vertex  $v$ . Early reject holds when two neighbours are not in shadow and do not cast shadow on  $v$ . For all other cases we need to test against further neighbours. Table 1 gives an overview of the performance of our shadow tests for different typical scenarios. The mean visited neighbourhoods (mvn) is the number of such tests in light direction. In the Alps scenario the medium shadow length of 11.91 tests (mvn) per shadow ray is much higher than in lowlands. This corresponds with the greater height of the peaks of terrain and the resulting longer shadows.

## 6 Atmospheric absorption

Lambert-Beer's law is used to get an estimate of the amount of energy absorbed on its way through the atmosphere ( $\Phi(h) = e^{-\lambda h}$ ). For an incoming solar constant of  $E_0 = 1367 \frac{W}{m^2}$  and known received energy measurements ( $E' = 1000 \frac{W}{m^2}$  at air mass  $\psi = 48.2^\circ$ ) we can derive a formula for an atmospheric correction factor and the corrected energy

Area	Grid points	Time	Early accept	Early reject	mvn
Alps	995 x 711	15.07. at 12 am	3,005	639,999	1.18
Alps	995 x 711	15.01. at 9 am	489,858	153,081	11.91
Lowland	995 x 711	15.07. at 12 am	0	702,336	1.002
Lowland	995 x 711	15.01. at 9 am	8,502	693,793	1.02

Table 1: The effect of early accept/reject tests: mean visited neighbourhoods

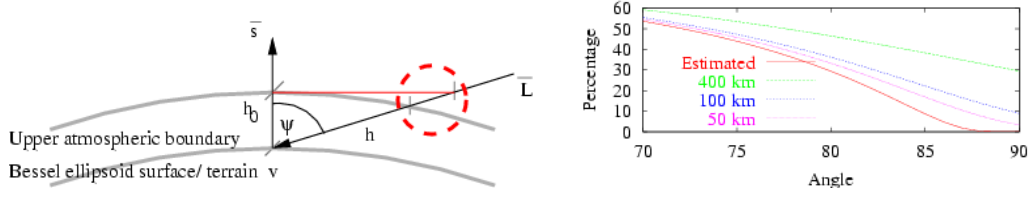


Figure 4: Approximation of traversed atmospheric length, Lambert-Beer factor for differing atmospherical thicknesses  $h_0$  (closeup for angles greater  $70^\circ$ )

$E_{\text{AtmosCorr}}(\vec{L}, v)$ . We simplify the traversed atmospheric length  $h$  to  $h = \frac{h_0}{\cos(\psi)}$  for computational speed.

$$E = E_0 \cdot \Phi(h) = E_0 \cdot e^{-\lambda h} = E_0 \cdot e^{-\frac{\lambda h_0}{\cos \psi}}$$

$$E_{\text{AtmosCorr}}(\vec{L}, v) = E_{\text{Lambert}}(\vec{L}, v) \cdot e^{-\frac{\lambda h_0}{\langle |\vec{s}|v \rangle}}$$

The errors introduced by this approximation are negligible due to the thinness  $h_0$  of the atmosphere compared to its curvature for small values of  $\psi$ . We retain stability in spite of the error because of the exponential function (see figure 4 right). Note that the traversed atmospheric length  $h$  does not have to be computed explicitly. For accuracy, we provide an exact calculation of the traversed atmospheric length in our tool as well. Traversed length is then given by

$$h = r \cos(\psi) + \sqrt{r^2 (\cos(\psi))^2 + 2 r h_0 + h_0^2}$$

and is dependent on the atmospherical thickness  $h_0$ . We implement this to fine-tune the model.

## 7 Results

To determine the sum of radiation we have to integrate the measurements distributed over the period of time that we observe. Our model can be evaluated at intervals specified by the

Sample time	Samples	Shadow time	Total time	Time/sample
15.07. 12 am	1	3.99 sec	5.25 sec	5.25 sec
15.01. 9 am	1	4.41 sec	5.61 sec	5.61 sec
March to October	3041	13, 332.15 sec	17, 283, 7 sec	5.68 sec

Table 2: Nürnberg TÜK 200 Region, 10, 071.2km<sup>2</sup>, 2, 222 x 1, 813 grid points

Sample time	Samples	Shadow time	Total time	Time/sample
15.07. 12 am	1	0.49 sec	0.87 sec	0.87 sec
15.01. 9 am	1	2.21 sec	2.49 sec	2.49 sec
March to October	3019	2, 853.44 sec	4, 500, 34 sec	1.49 sec

Table 3: Alps region (*Koralpe*) 1, 103km<sup>2</sup>, 888 x 497 grid points

user and the results are linearly interpolated for the given interval to form the integration. A typical region of interest for computation is about 10,000 km<sup>2</sup> in size and consists of roughly four million grid points (about the dimensions of the map TÜK 200, CC 7126 Nürnberg) or regions as small as 50 km<sup>2</sup>. We will give computation results for both lowland and mountainous regions. The samples taken indicate how often the model with its size in grid points was evaluated (hardware: P4, 3.6 GHz, 2GB RAM). Generally, a higher amount of work for shadow tracing results in longer rendering times per grid sample point. This is especially visible in the morning and evening hours of winter (see tables 2 and 3).

## 8 Validation and Significance

Our estimation of the direct radiation is too high compared with measurement data from meteorological stations. The reason is that we do not model indirect radiation (caused by e. g. clouds and fog) that is usually recorded separately. Diffuse radiation maps can be included as layers in GIS systems and thus can be combined with our data. Since the main aspect for the biologists is the accuracy of the interplay of terrain and radiation, our model is simple and robust enough to deliver convincing results for an upper boundary of radiation (high face validity). To increase the matching between measured data and our results, we refine our heuristic method for modelling the atmosphere and facilitate more control over that part of the system (iterative validation). By introducing absorption  $\alpha$ , transmission  $\tau$  and reflection  $\rho$  coefficients it is possible to find a solution trimmed by expert knowledge ( $\alpha + \tau + \rho = 1$ ). The model is based on the observation that  $\Phi(0) = 1 - \rho$  (pure reflection) and  $\Phi(h) = \tau$  (transmitted energy at depth  $h$ ). Again we estimate the traversed length  $h$  for speed and leave the exact computation optional.

$$E_{\text{AtmosCorr}}(\vec{L}, v) = E_{\text{Lambert}}(\vec{L}, v) \cdot (1 - \rho) \cdot \left( \frac{-\tau}{\rho - 1} \right)^{\frac{1}{\cos\psi}}$$

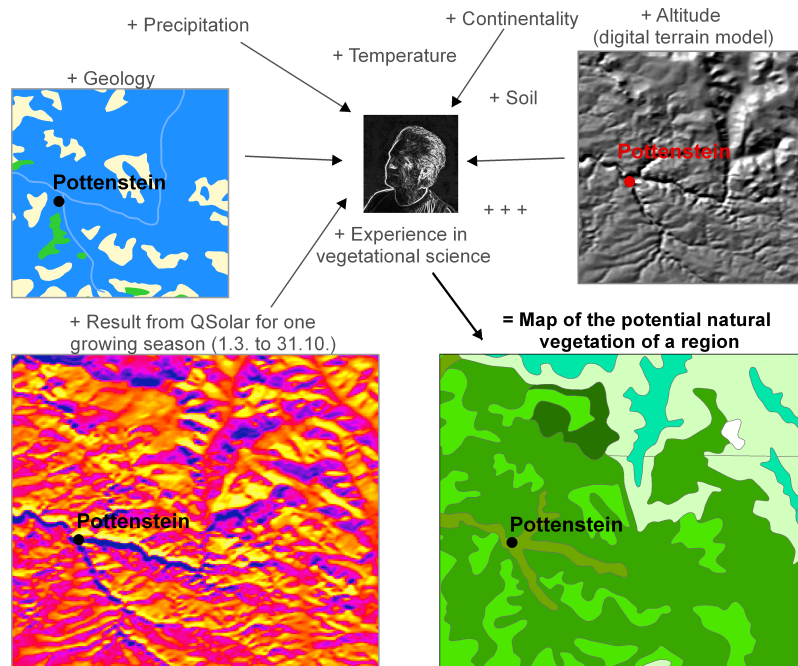


Figure 5: The different factors for IVL's PNV decision in the *Pottenstein* region (part of the *Fränkische Schweiz*, a region with an interesting relief. TÜK 200, CC 6634 Bayreuth)

## 9 Conclusion

We present a tool to compute maps of direct sun radiation in an interdisciplinary student project between computer graphics and IVL. We find a convincing, state-of-the-art model for representing the interdependencies of terrain and radiation with high face validity. The software is about to be extended to include different models for terrain other than pure diffuse reflection as it is used here. A more detailed and exact modelling of indirect radiation is a milestone for the future. Atmospheric effects including frequency dependencies and clouding with scattering of radiation are options for which computer graphics methods are available that can increase the validity of the model and the accuracy for PNV analysis.

## References

- [1] *Tüxen, R.*: Die heutige potentielle natürliche Vegetation als Gegenstand der Vegetationskartierung. *Angewandte Pflanzensoziologie* 13 (1956), S. 5-42.
- [2] *Hofmann-Wellenhof, B.*: GPS in der Praxis. Wien: Springer, 1994.
- [3] *Montenbruck, O., Pfleger, T.* Astronomy on the Personal Computer. Berlin: Springer, 2004
- [4] *Meeus, J.* Astronomical Algorithms. Willman-Bell, 1998